Reingestion and Footprint Characteristics of the VAK 191B

R. A. Weinraub*
Naval Air Systems Command, Washington, D. C.

During 1974 and 1975, the U.S. Navy and the Federal Ministry of Defense of the Federal Republic of Germany jointly flight tested the VFW-Fokker VAK 191B V/STOL aircraft. One of the primary objectives of this test program was to obtain full-scale reingestion and footprint data which could be directly compared with existing model scale data. An evaluation of the flight test data by the U.S. Navy and VFW-Fokker has demonstrated that the scaled-up model test results accurately predicted the reingestion and footprint characteristics of this aircraft. This paper summarizes the results of an investigation of the reingestion and footprint characteristics of the VAK 191B.

Nomenclature

b = wingspan, ft
CNT = counter number (time), s
D = exhaust nozzle exit diameter, ft
h = height of center-of-gravity above ground, ft
LE − F = front lift engine
LE − R = rear lift engine
ME = main engine
P = total pressure, psia
PSAC = aircraft azimuth angle, deg
P_N = nozzle exit pressure, psia
ΔP = $P - P_\infty$, psia
P_∞ = ambient pressure, psia
R = ground distance between rake and freejet impingement point, ft
T = total temperature, K
T/C = thermocouple
T_N = nozzle exit temperature, K
ΔT = $T - T_\infty$, K
$\overline{\Delta T}$ = average $(T - T_\infty)$, K (area average)
T_∞ = ambient temperature, K
ϑ = pitch attitude angle, deg
ϑ_N = T_N / T_∞
β = sideslip angle
σ = main engine nozzle angle, deg (nozzles oriented aft $\sigma = 0$, nozzles oriented vertically $\sigma = 90$)
σ_e = jet inclination angle relative to ground, deg
Π = P_∞ / P_N
γ = ratio of specific heats

Introduction

REINGESTION of hot gas into the inlets of a jet lift V/STOL aircraft, such as the VAK 191B (Fig. 1), can significantly reduce the amount of available engine thrust. A V/STOL aircraft's footprint characteristics will determine how that aircraft interfaces with ground personnel and equipment in an operational environment. Determination of the reingestion and footprint characteristics as early as possible in the conceptual development stages of a V/STOL aircraft is therefore essential from both a performance and operational standpoint. The VAK 191B flight test program, described in Ref. 1, provided the unique opportunity to compare predicted aircraft reingestion and footprint characteristics formulated during the early aircraft development stages against flight test data. A schematic diagram of the flowfield of the VAK 191B is presented in Fig. 2. These predictions of reingestion and footprint characteristics were based on extensive testing of a VAK 191B model. This test program is described in Ref. 2. The model was geometrically similar to the full-scale aircraft; however, the nozzle exit temperature and intake mass flow were significantly less than full-scale. A scaling methodology and an analytical flowfield description developed by R. Behnert[3] of VFW-Fokker was utilized to determine the reingestion and footprint characteristics of the full-scale aircraft. The validity of these scaling laws was demonstrated in Refs. 1 and 4. Representative comparisons of the predicted vs full-scale values of wall jet decay, fountain strength, and reingestion are presented in this paper.

Presented as Paper 77-617 at the AIAA/NASA Ames V/STOL Conference, Palo Alto, Calif., June 6-8, 1977; submitted June 13, 1977; revision received Dec. 27, 1977.

Index categories: Testing, Flight and Ground; Jets, Wakes, and Viscid-Inviscid Flow Interactions; Environmental Effects.

*Aerospace Engineer.

Instrumentation

The temperature instrumentation on the aircraft and on the model were placed in geometrically similar locations. Inlet reingestion on the aircraft was measured by 89 high-response thermocouples mounted on the debris guards of the main, auxiliary, and lift engine inlets. Six thermocouples were mounted on the bottom of the aircraft to measure the fountain temperature decay. Two ground rakes were constructed to measure the thermal and pressure footprint of the aircraft; one oriented along the runway centerline, the other perpendicular to it. These rakes contained 55 thermocouples and 43 pressure transducers. A schematic diagram of instrumentation locations is shown in Fig. 3. The output from this instrumentation was continuously recorded, along with pertinent aircraft information.

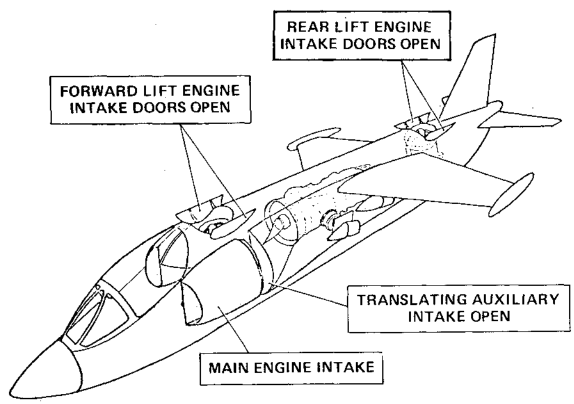

Fig. 1 VAK 191B V/STOL aircraft.

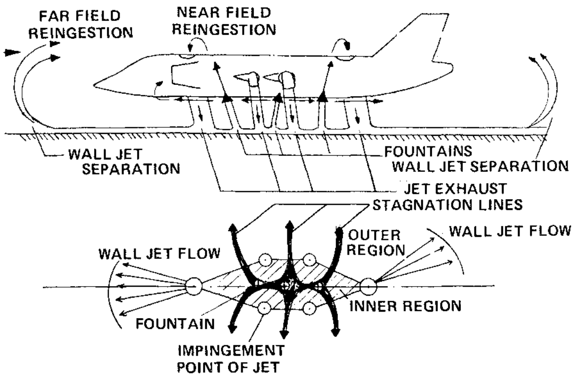

Fig. 2 VAK 191B flowfield.

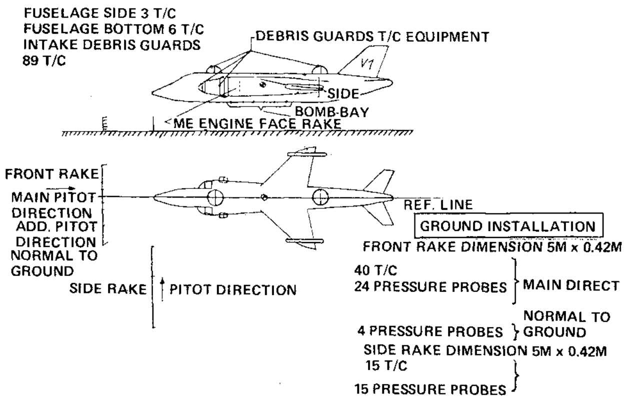

Fig. 3 Test instrumentation.

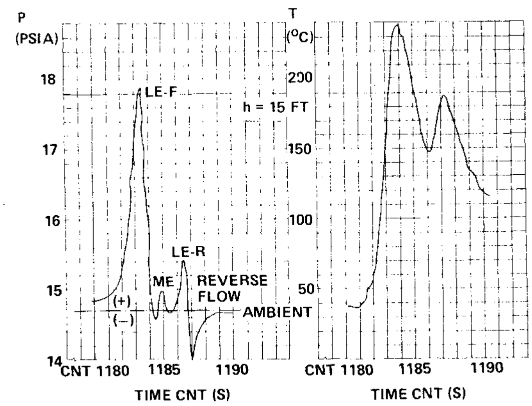

Fig. 4 Response of rake system.

The thermocouples located on the rake system and on the underside of the fuselage were subjected to high energy flow. These thermocouples were therefore constructed from a relatively heavy-gage wire. The time response characteristics of these heavier-gage thermocouples were longer than that desired for nonsteady-state testing. The relatively slow response of these thermocouples is demonstrated in the following example. In Fig. 4, the aircraft is flying slowly toward the rake system along the runway centerline with pressure and temperature presented as a function of time. As the aircraft passes over the rake system, the change in wall jet pressure due to the main and lift engines is clearly visible. The slower response characteristic of the temperature instrumentation prevents the same degree of resolution of the flowfield as the pressure instrumentation. During nonsteady-state testing, the output from the fuselage underside thermocouples and the rake system thermocouples and pressure transducers was corrected for time-response characteristic, using the methodology described in Ref. 1.

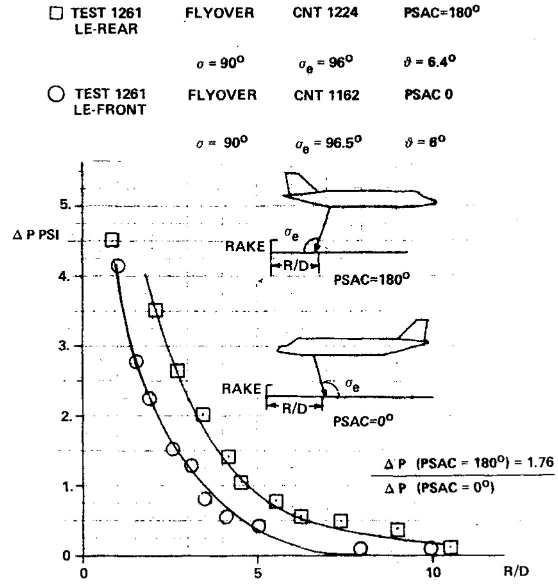

Fig. 5 Comparison of lift engine wall jet pressure decay for PSAC = 0 deg, 180 deg.

Wall Jet Decay/Footprint

The majority of the jet decay data presented in this section were obtained in the wall jet produced by front or rear lift engine. The data were obtained using either a flyover or ground test procedure. Prior to the U.S. Navy entry into the VAK 191B program, a limited amount of testing was conducted with the aircraft mounted on a pedestal (test stand). During flyover testing, the aircraft was flown (along the runway centerline) over the rake system or was hovered close to the rake system. An optical tracking device was used to locate the aircraft during flyover testing. Therefore, the distances between the jet impingement points and the individual rakes could be determined. This test procedure was extremely valuable for investigation of the wall jet in the region of high rate of decay of pressure and temperature. The ground testing was conducted with the aircraft located in fixed positions relative to the rake system. This test technique eliminated the problems of instrumentation response time and aircraft location associated with flyover testing. However, this method resulted in long periods (time $\simeq 12$ min) of hot exhaust impingement on the ground and external parts of the aircraft, thereby increasing the possibility of severe ground erosion and/or damage to the landing gear. Due to this problem, ground testing was limited to reduced power settings. It should be pointed out that this was a time-dependent problem and was not encountered during normal aircraft operations.

Reference 1 indicates that wall jet temperature and pressure decay can be described in the following manner

$$\frac{\Delta T}{\Delta T_N} = \left(1 - \frac{4}{\pi}\cos\sigma_e \cdot \cos(\mathrm{PSAC})\right) \cdot \frac{C_{W_1}}{\vartheta_N^{1/4} \cdot \Pi^{1/2} \cdot R/D} \qquad (1)$$

$$\frac{\Delta P}{\Delta P_N} = \left(1 - \frac{4}{\pi}\cos\sigma_e \cdot \cos(\mathrm{PSAC})\right)^2 \cdot \frac{C_{W_2}}{\vartheta_N^{1/4} \cdot \Pi^{(2\gamma - 1/2\gamma)} \cdot (R/D)^2} \qquad (2)$$

The influence of freejet inclination angle on wall jet decay can be demonstrated by comparing the wall jet decay for the case when the nose of the aircraft is pointed toward the rake system (azimuth angle PSAC = 0 deg) with the case of the aircraft tail pointed toward the rake system (PSAC = 180 deg). When the nose of the aircraft is pointed toward the rake

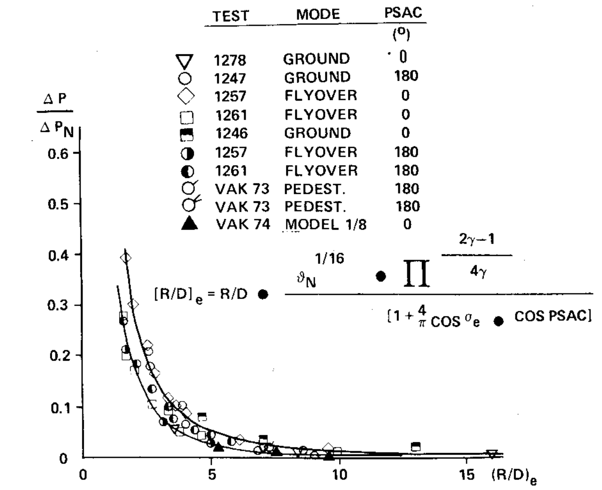

Fig. 6 Lift engine wall jet pressure decay.

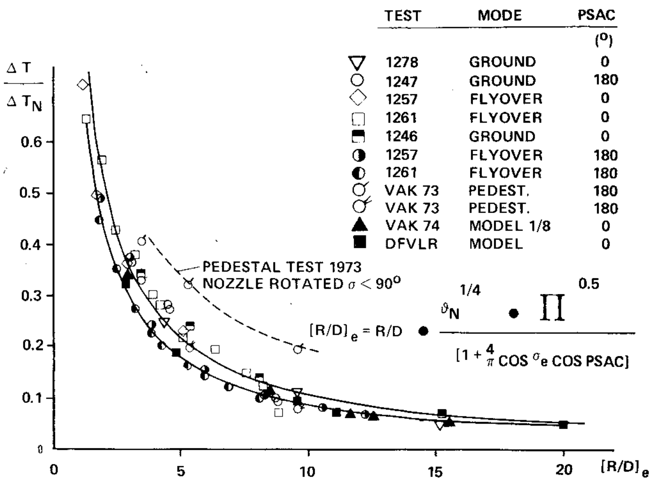

Fig. 7 Lift engine wall jet temperature decay.

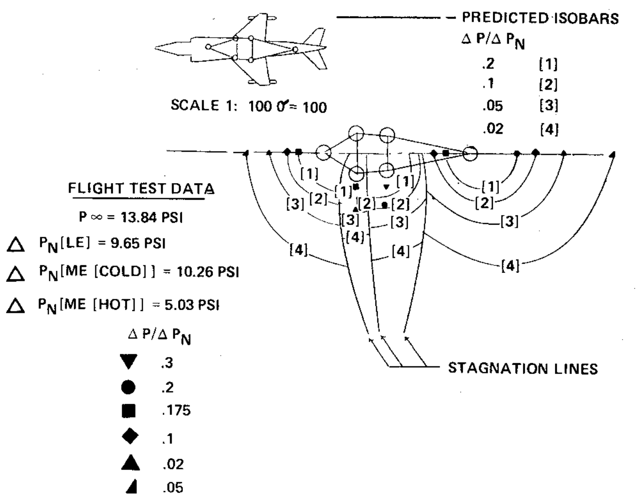

Fig. 8 Comparison of predicted and measured VAK 191B footprint.

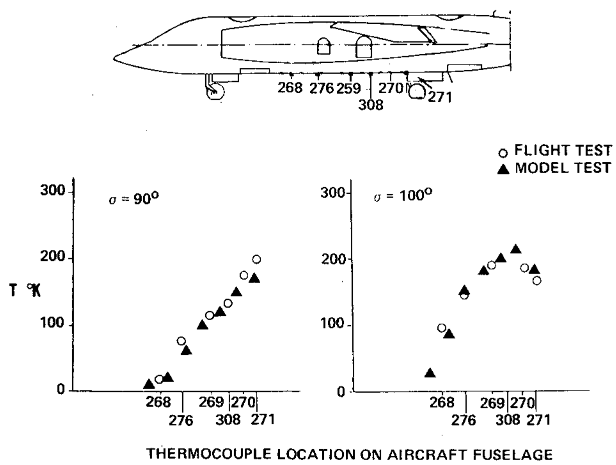

Fig. 9 Fuselage bottom temperature rise.

system (PSAC = 0 deg), the front lift engine exhaust must turn through a larger angle in order to reach the rake system than the rear lift engine exhaust when the tail of the aircraft is pointed toward the rake system (PSAC = 180 deg). Therefore, a higher rate of decay of the wall jet is expected for the case of PSAC = 0 deg than for PSAC = 180 deg. This point is illustrated in Fig. 5 for decay of the maximum pressure in the wall jet. Using Eq. (2) for the case shown in Fig. 5,

$$\frac{\Delta P(\mathrm{PSAC}=180\ \mathrm{deg})}{\Delta P(\mathrm{PSAC}=0\ \mathrm{deg})}=1.76$$

The data from Fig. 5 verifies this calculation in the region of high wall jet pressure decay.

The available full-scale and model wall jet decay data from the VAK 191B program are summarized in Figs. 6 and 7. All the test results, with the exception of one set of pedestal temperature tests, are clustered about two curves. The decay constants for these curves are: temperature – $0.88 \leq C_{W_1} \leq 1.11$; and pressure – $0.76 \leq C_{W_2} \leq 1.25$. It is evident from the correlation of the test data demonstrated in Figs. 6 and 7 that Eqs. (1) and (2) adequately describe the decay of the maximum pressure and temperature in the wall jet region.

An example of the footprint of the VAK 191B is shown in Fig. 8. The predicted isobars, which were developed using an analytical technique described in Ref. 1, are compared with flight test data. The measured pressure data compares well with the calculated isobars.

Fuselage Bottom Temperature

The high fuselage bottom temperatures associated with takeoff or landing operations are a result of fountain impingement on the bottom of the aircraft. These fountains are formed by interacting wall jets in the inner flow region shown in Fig. 2. Near-field reingestion and fuselage bottom temperature rise have the same physical origin – the fountain. Therefore, an understanding of the characteristics of the fountain and its interaction with the aircraft is essential if the phenomena of near-field reingestion is to be understood. The fuselage bottom temperature distribution provides information on fountain location, inclination, and decay.

Two examples of comparisons between flight test fuselage bottom temperatures and model data are presented in Fig. 9. The relationship between nozzle angle (freejet inclination angle) and fountain inclination is illustrated in this figure. The maximum value of fuselage bottom temperature corresponds to the location of the impingement point of the fountain formed by the rear main engine nozzles and the rear lift engine wall jets (see Fig. 2). As the main engine nozzles are rotated forward from 90 to 100 deg, the portions of wall jets moving in the aft direction from the main engine rear nozzle lose momentum. The forward-moving portion of the wall jet formed by the rear lift engine maintains constant momentum, and therefore the fountain formed by these interfering wall jets is inclined further forward.

Reingestion

Reingestion of hot exhaust gas into the inlets of an aircraft can be divided into two categories: near-field and far-field.

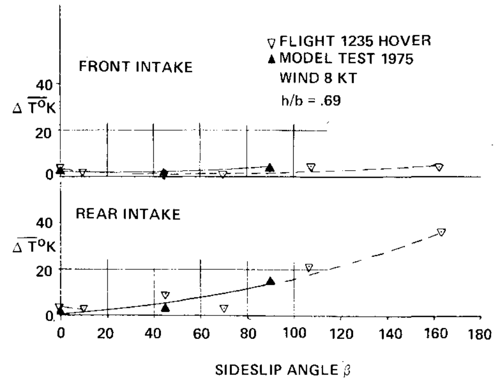

Fig. 10 Influence of sideslip on lift engine inlet temperature.

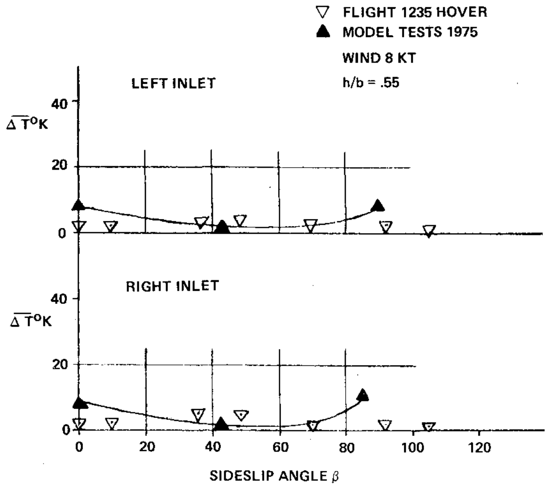

Fig. 11 Influence of sideslip on auxiliary inlet temperature.

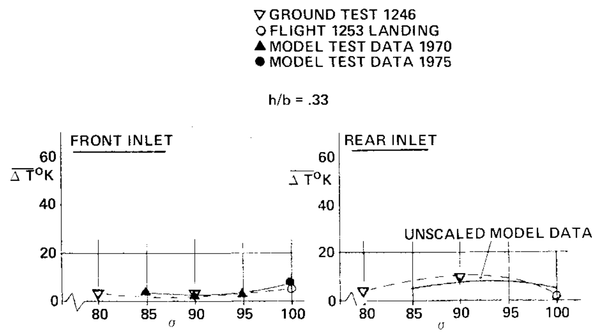

Fig. 12 Influence of nozzle angle on lift engine temperature rise.

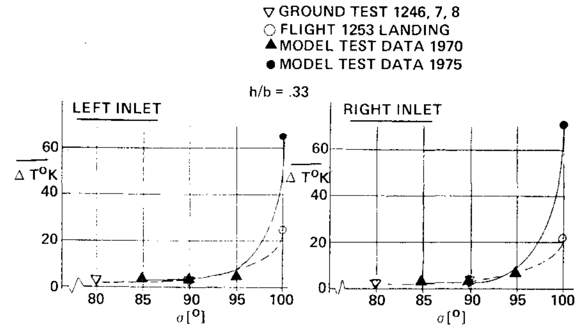

Fig. 13 Influence of nozzle angle on auxiliary inlet temperature.

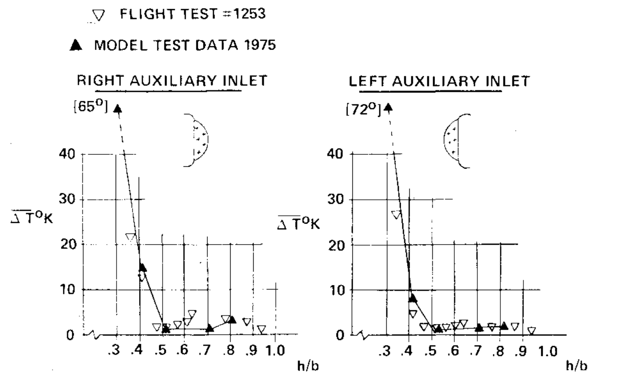

Fig. 14 Main engine auxiliary inlet temperature rise, landing, $\vartheta = 100$ deg.

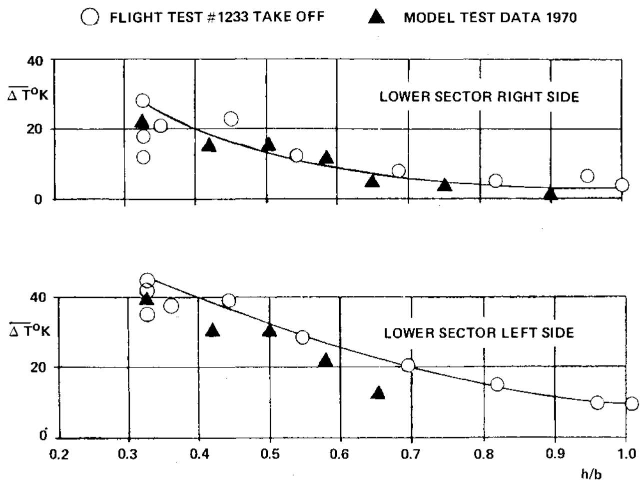

Fig. 15 Main engine inlet temperature rise, takeoff, $\sigma = 100$ deg.

Near-field reingestion is a result of the jet exhaust spreading and interacting on the ground beneath the aircraft. As illustrated in Fig. 2, fountains are formed from the interaction of wall jets in the inner region of the flowfield. If a fountain hits the aircraft in the vicinity of an inlet, reingestion may occur. By controlling the fountain positions within a multijet flowfield, it is possible to drastically reduce reingestion. The reingestion characteristics of the VAK 191B, presented in Figs. 10-16, are the result of near-field effects.

Parameters which can influence the position of the fountains and, therefore, near-field reingestion are:

1) The inclination angle of the freejet. This angle can be varied by rotating the main engine nozzles or changing the attitude of the aircraft.

2) The height of the aircraft above the ground. Variation of the aircraft altitude changes the location of the fountain impingement points on the aircraft.

3) Variation of the thrust distribution between the aircraft's engines. This changes the momentum balance between the wall jets in the inner region and, therefore, the fountain inclination angle.

Far-field reingestion is the result of hot exhaust gas from a separated wall jet entering an inlet. This concept is illustrated in Fig. 2. Wall jet separation can result from the interaction of a wall jet and the ambient wind or the dominance of buoyant forces within the wall jet. Far-field reingestion usually results in a lower inlet temperature rise than near-field reingestion, due to the relatively large distance from the wall jet separation point to the aircraft inlet. Significant far-field reingestion was not encountered during the VAK 191B flight test program.

It must be mentioned that during flight testing, the principle goal was to achieve the highest allowable temperatures in the intakes. Therefore, the high inlet temperatures displayed in this paper are not representative of the inlet temperature

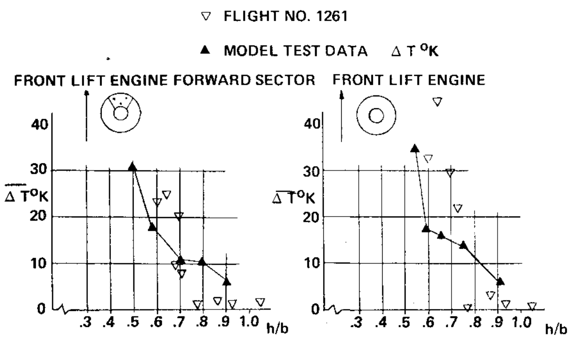

Fig. 16 Lift engine inlet temperature rise, hover, $\sigma = 100$ deg.

rise during normal aircraft operations, but are the result of deliberately flying the aircraft in regions associated with high inlet temperature rise for the purpose of comparison with specific model test points.

The reingestion characteristics of the lift engine inlets and main engine auxiliary inlets as a function of sideslip angle are presented in Figs. 10 and 11. The testing was conducted at low altitudes ($0.55 \leq h/b \leq 0.7$) in an 8-knot wind. It can be seen that sideslip angles up to 60 deg have a negligible influence on inlet temperature rise. The correlation between model and full-scale results is quite good in both trend and magnitude.

The influence of nozzle angle on the lift engine inlet and auxiliary inlet temperature rise is shown in Figs. 12 and 13. In this case, the aircraft is on the ground. As predicted by the model tests, Fig. 12 indicates that temperature level in the lift engine inlets is constant vs main engine nozzle angle. (Unfortunately, rear lift engine model temperature data suitable for scaling to the flight and ground test conditions displayed in Fig. 12 were not available. However, unscaled rear lift engine inlet temperature rise model data have been displayed in Fig. 12 in order to demonstrate that the model and full-scale aircraft exhibit the same trend as a function of main engine nozzle angle.) The high levels of temperature in the auxiliary inlets shown in Fig. 13 were produced by the forward inclination of a fountain when the main engine nozzles were swivelled forward to 100 deg. The high inlet temperature predicted by the model tests under these conditions (nozzle angle = 100 deg) was not verified during this test. The reason may be that the engine thrust was reduced by the pilot just prior to aircraft touchdown.

The trend, established during model testing, of vanishing reingestion for all inlets as the aircraft height increases above $h/b = 0.7$ was verified by the full-scale testing. Inlet reingestion, as a function of height above the ground for the auxiliary, main, and lift engines, is displayed in Figs. 14, 15, and 16. In Fig. 16, a comparison of flight test and model results in only the forward portion of the front lift engine inlet is shown, as well as a comparison of the average temperature rise for the entire inlet. Although the flight test data in Fig. 16 exhibit some scatter, the magnitude and trend of these test results correlate reasonably well with the corresponding model test data.

Conclusions

Representative VAK 191B flight test data were presented in order to prove the applicability of using model tests to predict the ground footprint and reingestion characteristics of the full-scale aircraft. The results obtained demonstrated good correlation between model predictions and flight test data. Wall jet and fountain decay were investigated under various power settings and jet inclination angles during ground and flyover testing. Full-scale testing verified the predicted decay charactertistics of the wall jets and fountains. Predicted isobars were found to correlate well with the measured full-scale pressure footprint data. A relatively small region of high jet blast around the VAK 191B was displayed. Accurate prediction of full-scale reingestion characteristics of individual inlets using scaled model testing was also demonstrated.

References

[1] Behnert, R. and Weinraub, R., "USN/FMOD FRG VAK 191B Joint Flight Test Program, Vol. 7, Footprint and Reingestion," Naval Air Systems Command Report, June 1977.

[2] Behnert, R. and Roekmojoto, R., "A Compendium of Recirculation Model Data for the VAK 191B," VFW-Fokker Report Ea 268, Oct. 1970.

[3] Behnert, R., Kleppe, K. H., and Roekmojoto, R., "Ground Effect During Jet Supported Vertical Take-Off," VFW-Fokker Report Ea 380, Aug. 1971.

[4] Barron, W. and Frauenberger, H., "Ground Footprint Theoretical and Experimental Studies," Naval Air Systems Command V/STOL Workshop Paper, July 1975.